Int J Earth Sci (Geol Rundsch) (2015) 104:909–925
DOI 10.1007/s00531-014-1127-1

ORIGINAL PAPER

The Late Neoproterozoic magmatism in the Ediacaran series of the Eastern Pyrenees: new ages and isotope geochemistry

J. M. Casas · M. Navidad · P. Castiñeiras · M. Liesa · C. Aguilar · J. Carreras · M. Hofmann · A. Gärtner · U. Linnemann

Received: 11 March 2014 / Accepted: 7 December 2014 / Published online: 23 December 2014

Abstract Geochronological U–Pb (LA-ICP-MS), geochemical and isotopic data from metavolcanic felsic rocks of the Canigó and Cap de Creus massifs in the Eastern Pyrenees provide evidence of an Ediacaran magmatic event lasting 30 Ma in NE Iberia. These data also constrain the age of the Late Neoproterozoic succession in the Cap de Creus massif, where depositional ages range from 577 to 558 Ma, and in the Canigó massif, where the data (575–568 Ma) represent minimum ages. The geochemistry of the felsic rocks indicates that they were formed in a back-arc environment and they record a fragment of a long-lived subduction-related magmatic arc (620–520 Ma) in the active northern Gondwana margin. The homogeneity shown by all these crustal fragments along this margin suggests that the individualization of the Pyrenean basement from the Iberian Massif started later, probably during its transition from an active to a passive margin in Cambro–Ordovician times.

Keywords Ediacaran magmatism · Pyrenees · Cadomian · U–Pb zircon geochronology · Sr–Nd isotopes

Introduction

Upper Neoproterozoic–lower Cambrian magmatic rocks have been extensively described in the Ediacaran sequences of several areas of the European Variscan Belt (Lescuyer and Cocherie 1992; Fernández-Suárez et al. 1998; Alexandrov et al. 2001; Gutiérrez-Alonso et al. 2004; Mingram et al. 2004; Teipel et al. 2004; Alexandre 2007; Melleton et al. 2010; Rubio-Ordónez et al. 2013) and in the Variscan basement rocks involved in the Mediterranean Alpine orogens (Cocherie et al. 2005; Micheletti et al. 2007; Castiñeiras et al. 2008; Williams et al. 2012; Fiannacca et al. 2013). These magmatic rocks, which constitute the most important evidence of the Cadomian orogeny in these areas, are associated with the later stages of the long-lived active margin that resulted from a Gondwana directed subduction of a former (Protothetys or Iapetus?) peri-Gondwanan ocean. These rocks also provide valuable information about the

Electronic supplementary material The online version of this article (doi:10.1007/s00531-014-1127-1) contains supplementary material, which is available to authorized users.

J. M. Casas (✉)
Departament de Geodinàmica i Geofísica-Institut de Recerca GEOMODELS, Universitat de Barcelona (UB), Martí i Franquès s/n, 08028 Barcelona, Spain
e-mail: casas@ub.edu

M. Navidad · P. Castiñeiras
Departamento de Petrología y Geoquímica, Universidad Complutense de Madrid, 28040 Madrid, Spain

M. Liesa
Departament de Geoquímica, Petrologia i Prospecció Geològica, Universitat de Barcelona (UB), Martí i Franquès s/n, 08028 Barcelona, Spain

C. Aguilar
Departamento de Geologia, Universidade Federal de Ouro Preto, Ouro Prêto, MG 35400-00, Brazil

J. Carreras
Departament de Geologia, Universitat Autònoma de Barcelona (UAB), 08193 Bellaterra (Cerdanyola Del Vallès), Spain

M. Hofmann · A. Gärtner · U. Linnemann
Senckenberg Naturhistorische Sammlungen Dresden, Museum für Mineralogie und Geologie, Sektion Geochronologie, Königsbrücker Landstraße 159, 01109 Dresden, Germany

northern continental margin of Gondwana during its transition from active to passive in Cambro–Ordovician times (Eguiluz et al. 2000; Neubauer 2002; Murphy et al. 2004; Simancas et al. 2004; Linnemann et al. 2007; Nance et al. 2010). In most cases, the geochemical and isotopic studies of these igneous rocks enable us to assess the age of the pre-Ordovician metasedimentary sequences and correlate them along the whole margin. Should these studies not be undertaken, the ages of these sequences would remain unresolved because of the intensity of the Variscan and/or the Alpine deformation and metamorphism, the lack of fossiliferous content and the absence of reference stratigraphic horizons (Gutiérrez-Alonso et al. 2004; Rodríguez-Alonso et al. 2004; Talavera et al. 2012). This is the case of the basement of the Pyrenees, where Ediacaran magmatic rocks are interbedded in or intrude into a thick pre-Silurian series and constitute the only age constraint for the lower segment of this sequence (Cocherie et al. 2005; Castiñeiras et al. 2008; Mezger 2010). This pre-Silurian material exhibits characteristics that hamper their correlation with the classic zones defined in the Iberian Massif, suggesting a different evolution during Ordovician times. In the Pyrenees, we can highlight the absence of a thick Early Ordovician detrital sequence, the presence of Late Ordovician magmatism, and the evidence of Ordovician deformation [see discussion in Navidad et al. (2010)]. These characteristics pose some interesting questions about when this divergent evolution started and about the position of the Ediacaran rocks of the Pyrenees in the Gondwana margin.

In order to discuss these topics, we present new geochemical, isotopic and geochronological data from Late Neoproterozoic magmatic rocks of the Canigó and Cap de Creus massifs of the Eastern Pyrenees. These data allow us to characterize the pre-Variscan geodynamic evolution of this segment of the northern Gondwana margin and help to understand the paleogeography of the northern margin of Gondwana in Ediacaran times.

Geological setting

The presence of pre-Variscan igneous rocks in the pre-Silurian basement rocks of the Pyrenees has been reported by Guitard and Laffitte (1956) and Cavet (1957). These authors described metavolcanic acid rocks with a porphyritic texture, known as *gneiss granulé* (granular gneiss). These rocks are located in the lower part of a thick (up to 5,000 m) unfossiliferous metasedimentary series. This series is composed of metapelites and metagreywackes interbedded with numerous layers of marbles, quartzites and calc-silicates and is cut by orthogneiss bodies. In the Canigó massif (Fig. 1), Guitard (1970), Casas et al. (1986), Ayora and Casas (1986) and Navidad and Carreras (2002) also described greenschists and amphibolites derived from basaltic lava flows, diabasic dikes and gabbro bodies mainly located in the middle and lower part of this succession (Fig. 2). The close location of metavolcanic acid and basic rocks indicates that this bimodal magmatism may be coeval. The age of this lower series in the Canigó massif has been studied by SHRIMP U–Pb analyses in zircon by Cocherie et al. (2005) and Castiñeiras et al. (2008). However, the amount of inherited zircon hampers a straightforward interpretation of the isotopic data, resulting in two contrasting ages of 581 and 560 Ma, respectively (Figs. 2, 3a; Table 1). In addition, several bodies of augen orthogneisses (up to 2,000 m thick) derived from Ordovician intrusives (Cocherie et al. 2005; Casas et al. 2010) are present in this lower part of the succession. In the neighboring Roc de Frausa massif (Fig. 1), metatuffs have been assigned a Late Neoproterozoic age (548.4 ± 8.4 Ma, SHRIMP U–Pb analyses on zircon; Castiñeiras et al. 2008) for the uppermost part of the succession. The Mas Blanc orthogneiss located in the lower part of the Roc de Frausa massif has yielded a Late Neoproterozoic age (560.1 ± 7.2 Ma, SHRIMP U–Pb analyses on zircon; Castiñeiras et al. 2008). Nevertheless, because of its intrusive character, it cannot be used to determine the age of the lowermost part of the series since it only provides a minimum depositional age. This succession is overlain by a 1,500-m thick rhythmic alternation of sandstones, siltstones and argillites, with no metavolcanic intercalations (Fig. 2). This upper segment was recently dated using an acritarch assemblage that yielded a Late Cambrian (Furongian) to Early Ordovician age (Casas and Palacios 2012).

In contrast, the Cap de Creus massif is mainly made up of a 1,000-m thick monotonous alternation of predominant metagreywackes, with subordinate metapelites and discontinuous layers of plagio-amphibolites, banded quartzites and marbles that correspond to the lower segment of the pre-Silurian sequence. Metabasites crop out at the bottom and in the middle part of this sequence, whereas metatuffs are mainly interstratified at the top (Figs. 2, 3b; Navidad and Carreras 1995). Metabasites derive from gabbro–dolerite intrusions and basaltic lens-shaped bodies, and metatuffs from Al-rich calc-alkaline rhyolites and rhyodacites (Navidad and Carreras 1995). Metatuffs are interbedded with carbonaceous black slates and marbles, and they yield a Late Neoproterozoic age (560.1 ± 10.7 Ma, SHRIMP U–Pb analyses on zircon; Castiñeiras et al. 2008; Table 1). The uppermost outcropping levels are conglomerates, siliciclastic sediments and carbonates with marked lateral changes (Losantos et al. 1997). In contrast with the Canigó massif, no large aluminous augen ortthogneiss bodies derived from Ordovician intrusives are present, and only a 200-m thick subaluminous subvolcanic orthogneiss body (the so-called Port gneiss; Carreras and Ramírez 1984) crops out at the bottom of the sequence. Its

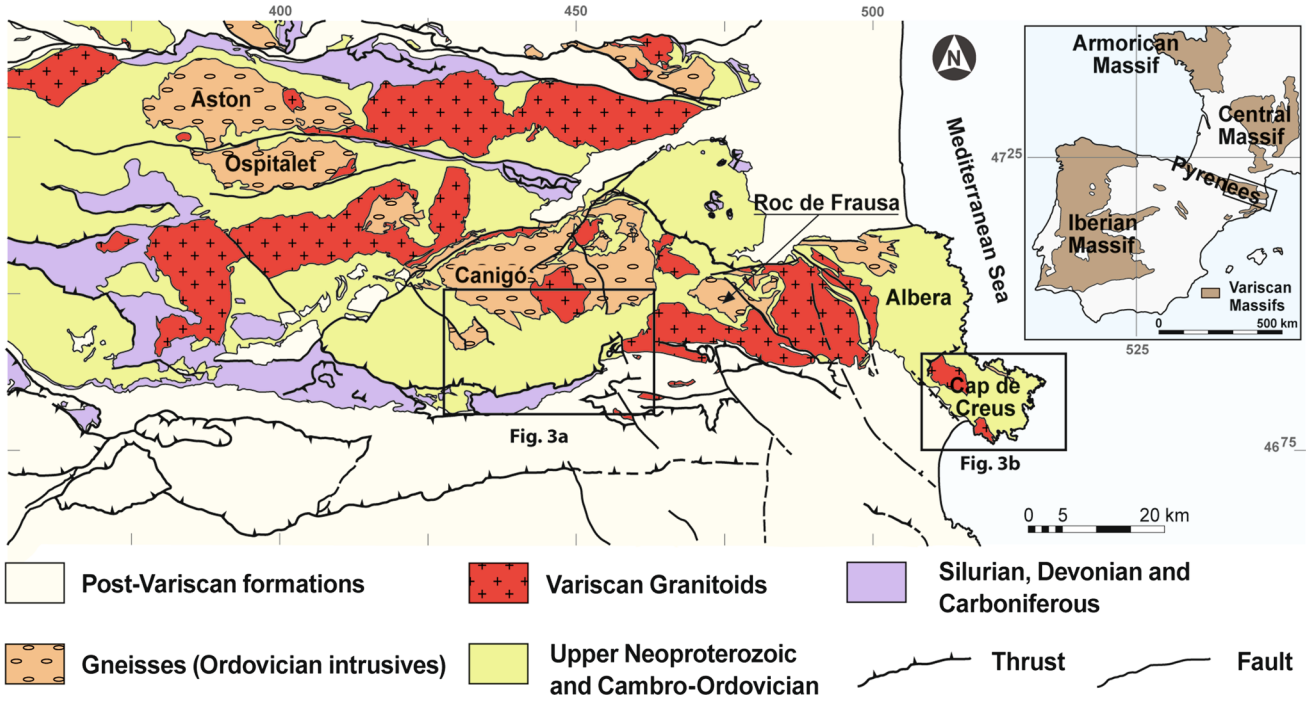

Fig. 1 Simplified geological map of the Eastern Pyrenees with the location of the Canigó and Cap de Creus massifs

protolith corresponds to a small intrusion of quartz-monzonite that yield 553 ± 4.4 Ma (SHRIMP U–Pb analyses on zircon; Castiñeiras et al. 2008; Table 1). Thus, the Port gneiss can be regarded as the plutonic equivalent of the metavolcanic rocks located in the upper part of the sequence.

A well-dated Upper Ordovician succession (Cavet 1957; Hartevelt 1970) lies unconformably over the Upper Neoproterozoic–lower Cambrian sequence (Santanach 1972a; García-Sansegundo and Alonso 1989; Den Brok 1989; Kriegsman et al. 1989; Casas and Fernandez 2007; Fig. 3a). Although the magnitude of this unconformity is not easy to evaluate, it may be assumed that there was considerable erosion before the Upper Ordovician deposition, because Upper Ordovician rocks overlie different sections of the pre-Upper Ordovician succession in the Central and Eastern Pyrenees (Santanach 1972a; Laumonier and Guitard 1986; Cirés et al. 1994; Muñoz et al. 1994). During the Silurian, black shales were deposited, which grade upwards to alternating black limestones and shales. The Devonian is represented by a limestone sequence, whereas the Carboniferous is made up of a detrital sequence (Culm facies) composed of slates with sandstones and conglomerates that unconformably overlie the aforementioned sequence.

Variscan deformation (Late Visean to Serpukhovian) accompanied by high-temperature–low-pressure metamorphism affected all these sequences (Guitard 1970; Zwart 1979). Syn- to late-orogenic granitoids (Late Bashkirian–Kasimovian, Romer and Soler 1995; Maurel et al. 2004; Aguilar et al. 2013 and references therein) intruded mainly into the upper levels of the succession. It should be noted that in the Pyrenees no tectono-metamorphic event related to the Cadomian orogeny has been described hitherto and that only a weakly developed Ordovician deformation (Mid to Late Ordovician in age) has been reported (Casas 2010), giving rise to folds without cleavage development and to normal faults. Finally, the Alpine cycle did not lead to a considerable penetrative deformation in the Variscan basement rocks (Muñoz 1992).

Sample description

Canigó massif

As stated above, the age of the lower sequence in the Canigó massif is constrained by radiometric data although the two U–Pb studies in zircon have yielded different ages. In order to better constrain the age of the interbedded volcanism and therefore the age of this succession, we selected three samples of acid metavolcanic rocks of the middle part of the series and three samples of metabasites of the lower part of the series on the southern slope of the massif (Figs. 2, 3a). Using the standard separation methods (see "Analytical methods" section), only the acid metavolcanic rocks yield zircons, and thus, the age of the lowermost part of the succession remains unresolved.

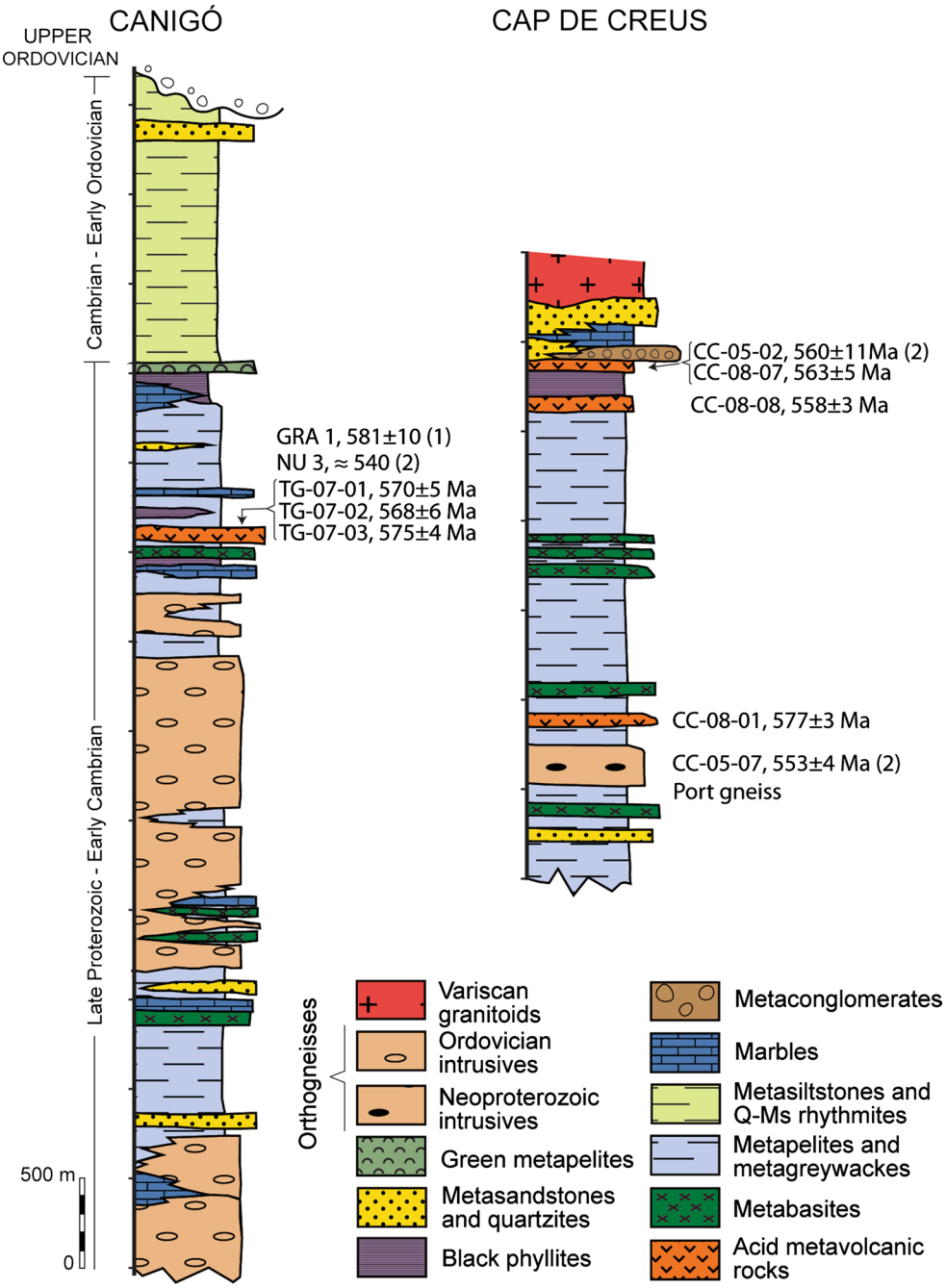

Fig. 2 Synthetic stratigraphic columns of the pre-Upper Ordovician rocks of the Canigó and Cap de Creus massifs with the location of the samples and previous geochronological data (1) Cocherie et al. (2005), (2) Castiñeiras et al. (2008). Stratigraphic data from Guitard (1970), Santanach (1972b), Ayora and Casas (1986) and Losantos et al. (1997)

Samples TG-07-01, TG-7-02 and TG-07-03 correspond to feldspathic metaignimbrites collected near the village of Tregurà, in an area where the metavolcanic rocks attain their maximum development (up to 500 m thick). These metavolcanic rocks are located in the same stratigraphic position as those studied by Cocherie et al. (2005) and Castiñeiras et al. (2008) (Figs. 2, 3a). They are overlain by black shales, sandstones and limestones of the upper part of the Late Neoproterozoic–Early Cambrian sequence and were previously described as conglomerates (Cirés et al. 1994). However, at outcrop and thin section scales, ample evidence of their volcanic origin can be detected. They are formed by heterometric fragments of volcanic rocks from 3 to 5 cm in size. The matrix is granular to mud-size with crystal fragments of feldspar and quartz resembling *gneiss granulé*, i.e., a metavolcanic porphyroid.

Sample TG-07-01 corresponds to an agglomeratic metatuff of dacitic composition. It is a heterogeneous rock formed by elongated fiammes (up to 10 cm in size), plagioclase and quartz porphyroclasts in a microcrystalline matrix. The fiammes are recrystallized to a fine-grained sericite aggregate. Plagioclase is subidiomorphic

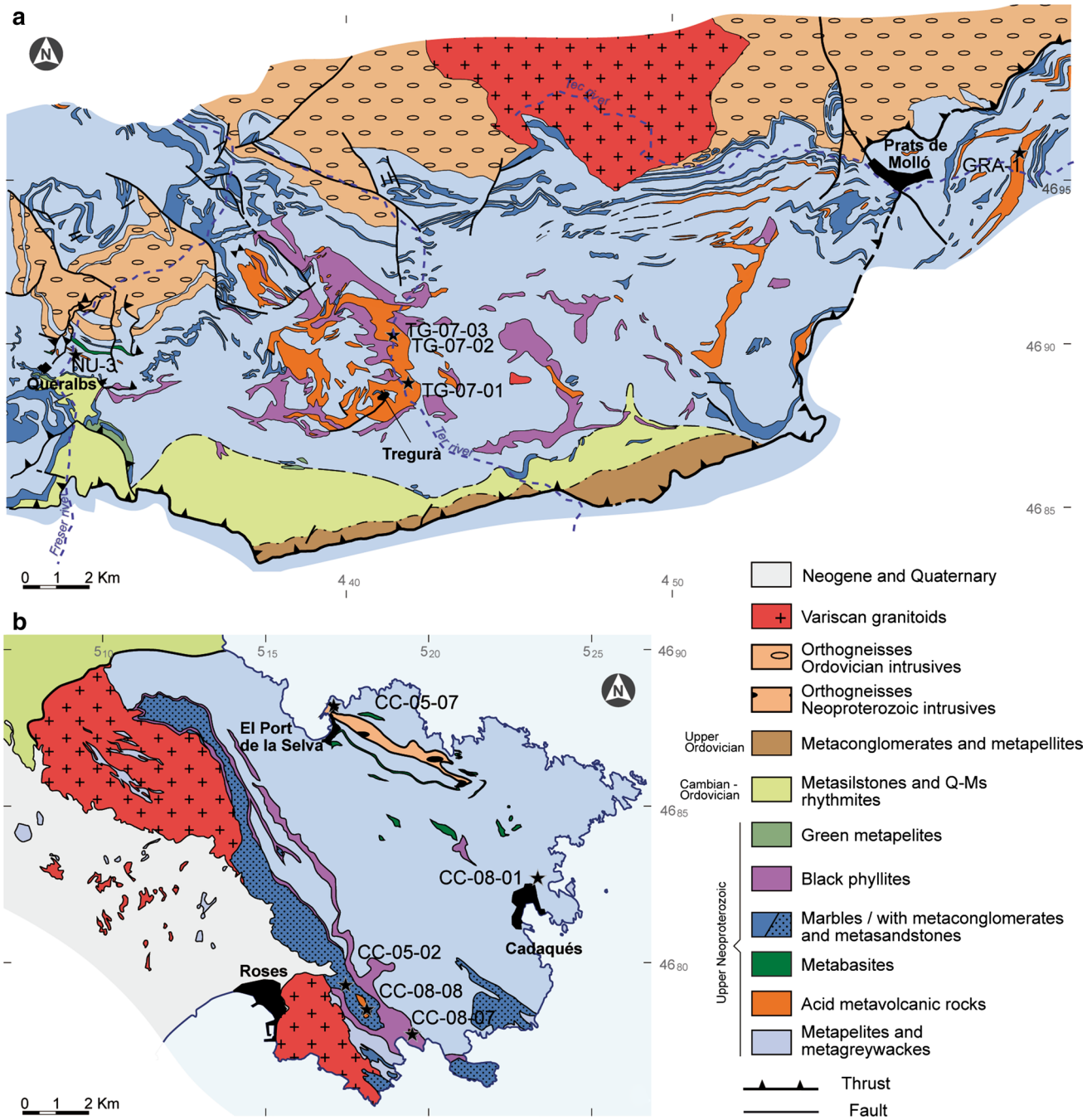

Fig. 3 Schematic geological maps with the location of our samples (TG-07-01, TG-07-02, TG-07-03, CC-01-01, CC-01-07 and CC-01-08) and previous geochronological data (GRA-1, Cocherie et al. 2005; NU-3, CC-01-02 and CC-01-07, Castiñeiras et al. 2008). **a** Southern flank of the Canigo massif and **b** Cap de Creus massif. Geological maps modified from Guitard (1970), Ayora and Casas (1986), Cirés et al. (1994), Muñoz et al. (1994) and Carreras and Druguet (2013)

to xenomorphic, and quartz is rounded and embayed. The matrix is mainly composed of quartz, feldspar, phengitic muscovite, chlorite and calcite. Zircon and ilmenite are the main accessory minerals. Replacements of K-feldspar by albite and myrmekitic quartz are frequent. Leucoxene, and locally titanite, replaces ilmenite. Leucoxene is generally associated with calcite, probably filling former vesicles. Two foliations can be observed, defined by secondary muscovite, chlorite and iron ore. The first foliation is folded, forming a well-developed axial plane foliation.

Sample TG-07-02 corresponds to a feldspathic metatuff with a porphyroid structure. Feldspar and quartz

Table 1 Geochronological data of samples of (1) Cocherie et al. (2005), (2) Castiñeiras et al. (2008) and this work

Sample	References	Rock type	Age	Sampling site	X	Y
GRA I	(1)	Acid metatuff	581 ± 10 (U–Pb SHRIMP)	Canigó massif. "Sitges" lapillis, D15 road left bank of Tec river, St. Eloi oratory	615,440	1,711,444
NU 3	(2)	Acid metatuff	≈ 540 (U–Pb SHRIMP)	Canigó massif. Queralbs-La Farga	431,759	4,689,782
RF 3	(2)	Acid metatuff	548 ± 8 (U–Pb SHRIMP)	Roc de Frausa massif. Les Illes. Mas Quintassos	481,970	4,696,770
RF 4	(2)	Mas Blanc gneiss	560 ± 7 (U–Pb SHRIMP)	Roc de Frausa massif. Mas Blanc	482,058	4,696,535
CC 2	(2)	Acid metatuff	560 ± 7 (U–Pb SHRIMP)	Cap de Creus massif. Roses. Coll d'Alzeda	517,736	4,679,447
CC 7	(2)	Port gneiss	553 ± 4 (U–Pb SHRIMP)	Cap de Creus massif. Port de la Selva quarry	517,582	4,687,795
TG-07-01	This work	Ignimbrite	570 ± 5 (LA–ICP–MS)	Canigó massif. Tregurà. GIV5284 road, left bank of Ter river	442,098	4,688,717
TG-07-02	This work	Ignimbrite	568 ± 5 (LA–ICP–MS)	Canigó massif. Tregurà. GIV5284 road, left bank of Ter river	441,882	4,689,874
TG-07-03	This work	Ignimbrite	575 ± 4 (LA–ICP–MS)	Canigó massif. Tregurà. GIV5284 road, right bank of Ter river	441,683	4,690,200
CC-08-01	This work	Acid metatuff	577 ± 3 (LA–ICP–MS)	Cap de Creus massif. Cadaqués. S'Alqueria Petita	523,965	4,682,985
CC-08-07	This work	Ignimbrite	563 ± 5 (LA–ICP–MS)	Cap de Creus massif. Cala Montjoi, Torre Morisca	519,401	4,678,026
CC-08-08	This work	Acid metatuff	558 ± 3 (LA–ICP–MS)	Cap de Creus massif. Roses-Cadaqués road. Mas de la Torre	518,226	4,677,333

porphyroclasts (1–2 mm in size) are embedded in a fine-grained foliated recrystallized groundmass made up of quartz, feldspar, chlorite, calcite and white mica with leucoxene and clinozoisite as accessory minerals. The groundmass exhibits abundant fiammes and glass shards recrystallized to sericite. Quartz porphyroclasts are locally embayed and recrystallized to subgrains.

Sample TG-07-03 is a feldspathic metatuff with fiammes similar to the samples described above. Under the microscope, it presents plagioclase and quartz porphyroclasts in a fine-grained recrystallized groundmass formed by aggregates of roughly equant quartz and feldspar. Rounded and embayed quartz is usually broken and welded by the matrix. Abundant ignimbrite textures are present in the matrix, such as glass shards and glass spherulitic textures replaced by leucoxene.

Cap de Creus massif

In the Cap de Creus massif, three acid metavolcanic rocks and three metabasites were sampled for U–Pb zircon analysis in order to determine the age of the bimodal magmatism and to better constrain the age of the Ediacaran sequence in this massif (Figs. 2, 3b). Again, no zircon was detected in the metabasites.

Sample CC-08-01 corresponds to a decimeter-thick meta-ash tuff located at the bottom of the sequence, whereas samples CC-08-07 and CC-08-08 are metaignimbritic tuff and metatuff, respectively, located on top of the succession (Fig. 2). Sample CC-08-01 is a very fine-grained amphibolic leucogneiss and corresponds to an meta-ash tuff of trachyandesitic composition. It has a porphyroclastic texture with a granolepidoblastic groundmass. The metamorphic mineral assemblage is quartz, albite and white mica, stilpnomelane and scarce green amphibole (edenitic hornblende) with zircon, tourmaline, leucoxene and iron ore as accessory minerals. Quartz and feldspar (mostly plagioclase) porphyroclasts range between 0.1 and 0.2 mm in size. They have a rounded to elongated shape with subidioblastic habit. Polysynthetic twinning is abundant in plagioclase and some feldspar crystals also present Carlsbad twinning. Porphyroclasts are wrapped by white mica defining the main foliation.

Sample CC-08-07 corresponds to an andesitic metaignimbritc tuff with porphyroclastic texture and a grano-lepidoblastic matrix. Porphyroclasts are scarce and are mainly formed by plagioclase. They range between 0.2 and 0.3 mm in size, though some crystals attain 1 mm. The groundmass is grano-lepidoblastic and is composed of quartz, white mica, actinolite, chlorite, titanite and calcite. Plagioclase is partly replaced by clinozoisite. Muscovite defines a foliation. Ignimbritic textures are recognized as glass shards and fiammes recrystallized to sericite.

Sample CC-08-08 corresponds to a metatuff of dacitic composition. It has a porphyroclastic texture in a very fine-grained groundmass. The metamorphic mineral assemblage is formed by quartz, albite and chlorite with leucoxene, zircon and ilmenite as accessory minerals. Porphyroclasts (up to 2 mm in size) are composed of quartz and of plagioclase with polysynthetic twinning fragmented and welded by the matrix. The groundmass is formed by recrystallized quartz and feldspar and by newly formed metamorphic chlorite exhibiting a preferred orientation. Chlorite also crystallizes in pressure shadows around the porphyroclasts.

Analytical methods

Whole-rock geochemistry

Whole-rock analyses were carried out using ICP-OES (inductively coupled plasma optical emission spectrometry) for major and minor elements, and ICP-MS (inductively coupled plasma mass spectrometry) for trace elements at the Spectrochemical Laboratory of the Centre de Recherches en Pétrographie et Géochimie of Nancy (France). Whole-rock powders were prepared by fusion with $LiBO_2$ and HNO_3 dissolution. Precision and accuracy were both found to be better than 1 % (mean 0.5 %) for major and minor elements, 5 % for Cr, U, V and Zn and 10 % for Ni and Cu. This is corroborated by international standards and analysis of replicate samples (Carignan et al. 2001). Results are given in Table 2.

Sr–Nd isotopes

Sr–Nd isotope analyses were performed at the Geochronology and Isotope Geochemistry Centre of the Complutense University (Madrid, Spain) using ID-TIMS, in a sector 54 VG-Micromass Multicollector Spectrometer. Whole-rock samples were dissolved in ultra-pure reagents, and the isotopes were subsequently isolated by exchange chromatography. Measured isotopic ratios were normalized to $^{87}Sr/^{86}Sr = 0.1194$ and $^{143}Nd/^{144}Nd = 0.7219$ in order to correct mass fractionation. Errors are quoted throughout as two standard deviations from measured or calculated values. The decay constants used in calculations are the values $\lambda^{87}Rb = 1.42 \times 10^{-11}$ and $\lambda^{147}Sm = 6.54 \times 10^{-12}$ year^{-1}, recommended by the IUGS Subcommission for Geochronology (Steiger and Jäger 1977). Analytical uncertainties are estimated to be 0.01 % for $^{87}Sr/^{86}Sr$ ratios, 0.006 % for $^{143}Nd/^{144}Nd$ ratios and 1.0 and 0.1 % for the $^{87}Rb/^{86}Rb$ and $^{147}Sm/^{144}Nd$ ratios, respectively. Epsilon-Nd (εNd) values (Jacobsen and Wasseburg 1980) were calculated relative to a chondrite present-day $^{143}Nd/^{144}Nd$ value 0.51262 and $^{147}Sm/^{144}Nd$ of 0.1967. Replicate analyses of the NBS-987 Sr-isotope standard yielded an average $^{87}Sr/^{86}Sr$ ratio of 0.710250 ± 0.00004 ($n = 638$). One hundred and ninety-five analyses of the Johnson and Mathey Nd-standard over 1 year gave a mean $^{143}Nd/^{144}Nd$ ratio of 0.511854 ± 0.00003. The Sr–Nd isotope results are shown in Table 3.

Zircon geochronology

The volcanic nature of the analyzed samples gives rise to a large amount of inherited zircon, hampering so far the accurate dating of these rocks in the Canigó massif (Cocherie et al. 2005; Castiñeiras et al. 2008). To overcome this problem, we use the LA-ICP-MS technique (Laser Ablation, Inductively Coupled Plasma Mass Spectrometry) to analyze the U, Th and Pb isotopes in zircon, since we can obtain more data than in the previously used techniques and improve the accuracy of the age, even if this accuracy is at the expense of some precision. The analyses were carried out at the Museum für Mineralogie und Geologie (Senckenberg Naturhistorische Sammlungen Dresden), using a Thermo-Scientific Element 2 XR sector field ICP–MS coupled to a New Wave UP-193 Excimer laser system. The results of the zircon analyses are shown in Online Resource 1. Zircon concentrates were separated from 2 to 4 kg sample material at the Departamento de Petrología y Geoquímica (Universidad Complutense, Madrid). The fresh samples were crushed in a jaw crusher, ground in a disc mill and sieved to obtain the fraction below 150 µm. The heavy mineral fraction was concentrated using the Wilfley table, followed by magnetic separation in a Frantz isodynamic separator. The resulting non-magnetic fraction was further enriched using heavy liquids (methylene iodide). Final selection of the zircon grains for U–Pb dating was achieved by handpicking under a binocular microscope. Owing to the abundance of zircon in the sediments that melted to generate the volcanic rocks, there was an increased variety in zircon grain sizes, morphological types and colors. However, we selected the most idiomorphic and transparent types, trying to avoid inherited grains, broken crystals and inclusions. In spite of the measures taken, we expected in this final separate a moderate content in inherited grains. The zircon grains were mounted in resin blocks, polished to half their thickness and imaged with transmitted and reflected light on a petrographic microscope as well as with cathodoluminescence on a JEOL JSM-840 electron microscope (housed at the Centres Científics i Tecnològics of the Universitat de Barcelona) to identify internal structures, inclusions, fractures and physical defects.

A teardrop-shaped, low-volume laser cell constructed by Ben Jähne (Dresden) and Axel Gerdes (Frankfurt/M.) was used to enable sequential sampling of heterogeneous grains (e.g., growth zones) during time-resolved data

Table 2 Whole-rock geochemistry of the samples from the Canigó and Cap de Creus massifs

	CC-08-01	CC-08-07	CC-08-08	TG-07-01	TG-07-02	TG-07-03
SiO_2	69.25	58.98	55.79	66.86	68.61	55.57
TiO_2	1.33	0.61	1.30	0.75	0.73	0.67
Al_2O_3	14.28	9.74	19.00	12.84	12.18	11.71
$Fe_2O_{3(T)}$	3.71	4.31	7.64	5.03	4.52	4.34
MnO	0.03	0.15	0.10	0.12	0.09	0.13
MgO	1.08	3.72	3.21	2.38	1.98	1.85
CaO	1.07	11.30	1.33	1.94	2.40	10.35
Na_2O	2.13	2.14	7.54	2.58	2.59	2.48
K_2O	3.12	1.48	0.41	2.35	2.23	2.01
P_2O_5	0.17	0.17	0.37	0.25	0.20	0.25
LOI	3.22	7.46	2.66	3.56	3.44	9.68
Total	99.38	100.05	99.34	98.64	98.97	99.05
Ba	1,405	278	283	643	637	697
Be	1.8	<LD	<LD	1.8	1.6	<LD
Co	2.0	7.7	17	10	10	11
Cr	145	58	83	75	71	61
Cu	24	10	69	26	17	20
Ga	19	12	12	17	15	15
Hf	11	4.4	9.3	5.0	5.3	5.1
Nb	14	7.0	15	10	10	8.8
Ni	11	22	33	29	27	26
Rb	93	41	10	70	60	61
Sr	148	141	201	65	96	149
Ta	1.2	0.6	1.4	0.9	0.8	0.8
Th	13	6.9	16	10	10	9.1
U	3.8	1.9	4.1	2.4	2.2	2.5
V	137	57	113	77	75	71
Y	17	22	47	31	25	30
Zn	28	57	69	71	34	59
Zr	457	160	350	186	195	189
La	35	23	47	29	28	28
Ce	71	48	97	59	58	57
Pr	8.2	5.6	11.8	7.1	6.6	7.0
Nd	30	22	47	28	26	28
Sm	5.4	4.6	10	6.0	5.4	6.0
Eu	0.98	0.96	1.59	1.27	1.09	1.23
Gd	3.9	4.2	8.9	5.6	4.8	5.4
Tb	0.58	0.67	1.41	0.88	0.74	0.89
Dy	3.3	4.0	8.5	5.3	4.4	5.2
Ho	0.65	0.80	1.70	1.04	0.89	1.03
Er	2.0	2.2	4.9	2.9	2.5	2.9
Tm	0.33	0.34	0.74	0.43	0.37	0.43
Yb	2.5	2.3	5.0	2.8	2.5	2.9
Lu	0.42	0.34	0.76	0.42	0.39	0.43

Oxides expressed as wt%, minor and rare earth elements as ppm. $Fe_2O_{3(T)}$ expressed as total iron

LOI Lost on ignition, *<LD* below detection limit

acquisition (Frei and Gerdes 2009). Each analysis consisted of approximately 15-s background acquisition followed by 30-s data acquisition, using a laser spot-size of 25 and 35 µm, respectively. A common Pb correction based on the interference- and background-corrected ^{204}Pb signal and a model Pb composition (Stacey and Kramers 1975) was carried out when necessary. The necessity of the correction is judged on whether the corrected $^{207}Pb/^{206}Pb$ lies outside of

Table 3 Sr–Nd isotopic data

Samples	Sm/Nd	Rb/Sr	$(^{147}Sm/^{144}Nd)$	$(^{87}Sr/^{86}Sr)_P$	$(^{87}Sr/^{86}Sr)_{560}$	$(^{143}Nd/^{144}Nd)_P$	$(^{143}Nd/^{144}Nd)_{560}$	eNd_{560}	eSr_{560}	TDM (Ga)	Age (Ma)
TG-07-01	0.21	1.08	0.1284	3.121498	0.699797	0.512181	0.511709	−4.0	−57	1.52	570
TG-07-02	0.21	0.62	0.1275	1.806548	0.708024	0.512146	0.511679	−4.6	59	1.56	568
TG-07-03	0.22	0.41	0.1301	1.185574	0.707653	0.512175	0.511698	−4.3	54	1.55	575
CC-08-01	0.18	0.63	0.1083	1.812453	0.704474	0.512281	0.511884	−0.6	9	1.12	577
CC-08-07	0.21	0.29	0.1266	0.834941	0.709730	0.512159	0.511695	−4.3	84	1.52	571
CC-08-08	0.21	0.05	0.1284	0.141754	0.712765	0.512223	0.511752	−3.2	127	1.45	558

the internal errors of the measured ratios. Discordant analyses were interpreted with care. Raw data were corrected for background signal, common Pb, laser-induced elemental fractionation, instrumental mass discrimination, and time-dependant elemental fractionation of Pb/Th and Pb/U using an Excel® spreadsheet program developed by Axel Gerdes (Institute of Geosciences, Johann Wolfgang Goethe-University Frankfurt, Frankfurt am Main, Germany). Reported uncertainties were propagated by quadratic addition of the external reproducibility obtained from the standard zircon GJ-1 (~0.6 and 0.5–1 % for the $^{207}Pb/^{206}Pb$ and $^{206}Pb/^{238}U$, respectively) during individual analytical sessions and the within-run precision of each analysis. Concordia diagrams (2σ error ellipses), ages and relative probability plots were produced using Isoplot/Ex 2.49 (Ludwig 2001). The $^{207}Pb/^{206}Pb$ age was taken for interpretation for all zircons >1.0 Ga, and the $^{206}Pb/^{238}U$ ages for younger grains. For further details on analytical protocol and data processing, see Gerdes and Zeh (2006), Frei and Gerdes (2009) and Linnemann et al. (2014). Zircons showing a degree of concordance in the range of 90–110 % in this paper are classified as concordant because of the overlap of the error ellipse with the concordia. Th–U ratios are obtained from the LA-ICP-MS measurements of investigated zircon grains. U and Pb content and Th/U ratio were calculated with respect to the GJ-1 zircon standard and are accurate to approximately 10 %. In this work, a zircon population is composed of more than three concordant zircon grains.

Results

Whole-rock geochemistry

Felsic metaignimbritic tuffs and ashes have been classified using conventional diagrams for presumably modified rocks based on trace elements, such as Zr/Ti versus Nb/Y (Winchester and Floyd 1977) and Th versus Co (Hastie et al. 2007; Fig. 4). Most of the samples cluster along the line between the andesite and dacite–rhyodacite fields (Fig. 4a) or inside the dacite-rhyolite (Fig. 4b), depending on the diagram used. In the Hastie et al. (2007) diagram, the samples also plot in the high K calc-alkaline domain (Fig. 4b).

A trace element diagram normalized to the ORG (Harris et al. 1986) is presented in Fig. 5a. All the samples show similar profiles characterized by an enrichment of the mobile elements (K, Rb, Ba, Th, excepting sample CC-08-08) and a negative Ta–Nb anomaly. They also show a relative enrichment of Ce, Zr, Hf and Sm with respect to Y and Yb. These patterns are characteristic of the calc-alkaline and shoshonite series in volcanic arcs (Pearce et al. 1984).

In a REE chondrite-normalized (Taylor and McLennan 1985) diagram (Fig. 5b), the patterns are very similar. All the samples are enriched in light REE (LREE) with respect to the heavy REE (HREE) and show a moderate fractionation (with LREE/HREE ratios between 6.5 and 11) and a slight negative Eu anomaly (Eu/Eu* between 0.52 and 0.65). These patterns are typical of rocks with feldspar fractionation and without the participation of garnet. In the Cap de Creus samples, it is important to note that CC-08-01 and CC-08-07 (amphibole-bearing tuffs) are more depleted in total REE ($\Sigma REE = 165$ and 119, respectively) than CC-08-08, a non amphibolic ignimbrite with $\Sigma REE = 246$.

As regards the geodynamic setting, most of the samples plot between the volcanic arc and the within-plate fields in a Hf-Rb/30-Tax3 diagram (Harris et al. 1986; Fig. 6).

Isotopic geochemistry

The analyzed samples show a variation in $(^{87}Sr/^{86}Sr)_{560}$ ratios between 0.699797 and 0.712765 (Table 3). The lowest value in sample TG-07-01 clearly indicates a disturbance of the Rb–Sr isotopic system. The rest of the samples have plausible initial isotopic ratios, but these results are not considered for discussion owing to the sensitivity of the Rb–Sr system to disturbance. In contrast, the $(^{143}Nd/^{144}Nd)_{560}$ ratios are more uniform, varying between 0.511679 and 0.511884 (Table 3). For the epsilon notation, all samples were normalized to an age of 560 Ma. The εNd values were moderately enriched for most of the samples (below −4.0), with the exception of samples CC-08-01 and CC-08-08, which have less enriched values of −0.6 and −3.2, respectively (Fig. 7; Table 3). Extrapolation of

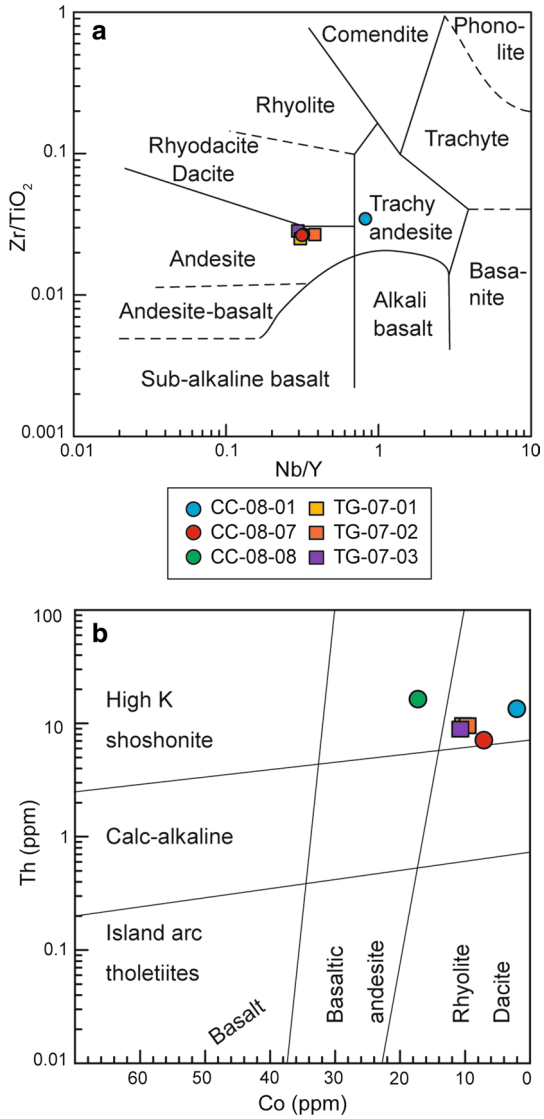

Fig. 4 **a** Zr/TiO_2 versus Nb/Y classification diagram (Winchester and Floyd 1977); **b** classification and character of the magma series in the Th–Co diagram (Hastie et al. 2007)

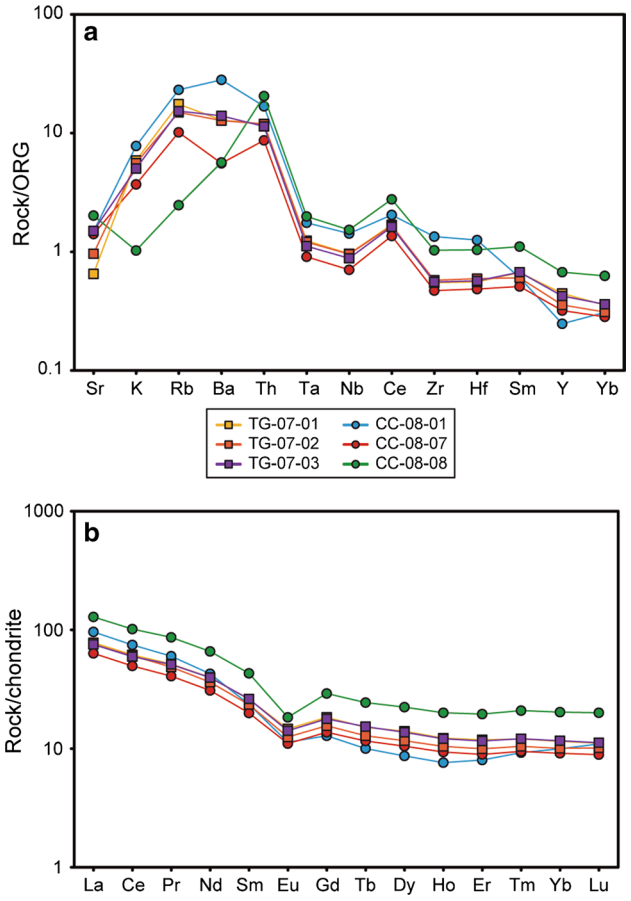

Fig. 5 **a** Multi-element diagram normalized to ORG values after Harris et al. (1986) and **b** chondrite-normalized REE diagram for the rocks [normalization values after Taylor and McLennan (1985)]

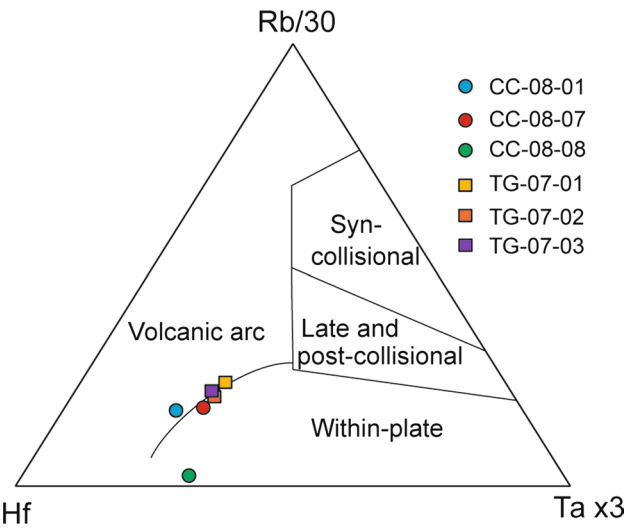

Fig. 6 Tectonic setting discrimination diagram after Harris et al. (1986)

εNd data back to the depleted mantle curve yield TDM values that are relatively homogeneous in the Canigó samples, varying between 1.52 and 1.56; in contrast, the Cap de Creus samples show more dispersed TDM values, from 1.12 through 1.52 (Fig. 7; Table 3).

Zircon geochronology

Under cathodoluminescence (CL), most zircons from the Canigó samples exhibit oscillatory zoning, with scarce xenocrystic cores or metamorphic rims. Some zircon grains with homogeneous textures can be found (Fig. 8). We

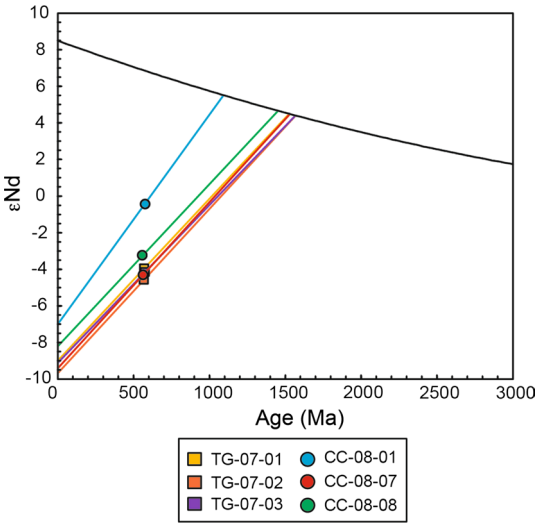

Fig. 7 εNd versus age diagram. Depleted mantle evolution calculated according to DePaolo (1981)

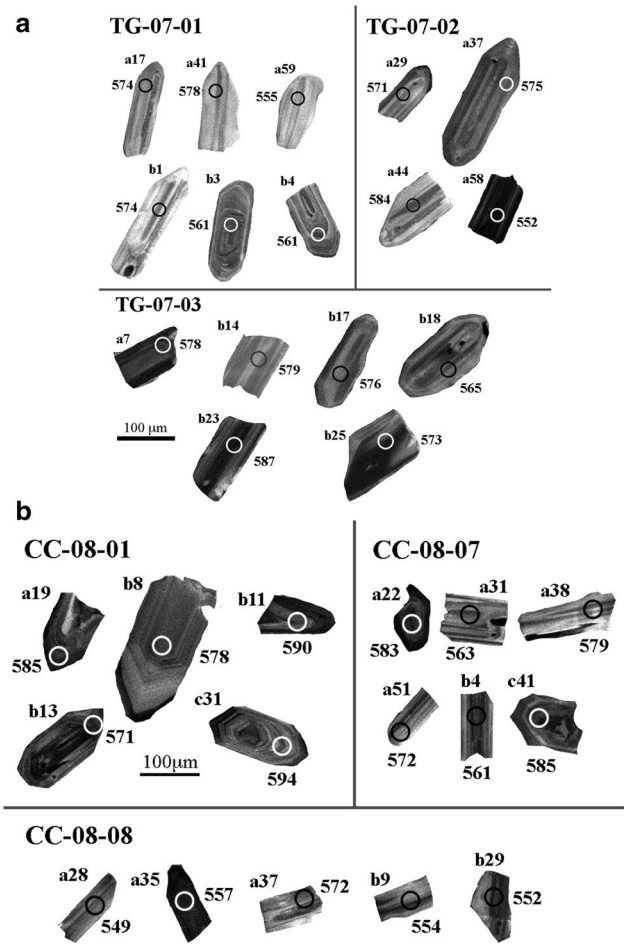

Fig. 8 Cathodoluminescence images for selected zircons from the analyzed samples

carried out a total of 184 analyses in as many zircon grains from the three Canigó samples selected. We disregarded 22 analyses with discordance higher than 10 %. In spite of our efforts to avoid inheritance during the handpicking of the zircon grains, the remaining 162 analyses are dispersed between 546 and 2,640 Ma. Obtaining a crystallization age from that dataset is a challenging task as three possibilities would concur, (1) the real age is at the younger end and the rest of the ages are considered inheritance, (2) the real age is at the older end and the rest of the ages are affected by some sort of lead loss, and (3) the real age is somewhere in the middle and the remaining ages are either affected by lead loss or are regarded as inheritance. Taking into account the concordance of the young ages and the results obtained for similar rocks in previous studies (Cocherie et al. 2005; Castiñeiras et al. 2008), we consider that the first aforementioned possibility is the one that better describes our case. Accordingly, we have selected the younger analyses to calculate the crystallization ages using the statistical methods available in Isoplot (Ludwig 2001).

In sample TG-07-01, eleven analyses vary between 555 and 588 Ma, yielding a concordia age (sensu Ludwig 1998) of 569.7 ± 4.8 Ma (Fig. 9a), with a mean square of weighted deviation (MSWD) of 0.43. In sample TG-07-02, nine analyses vary between 546 and 587 Ma, yielding a concordia age of 567.8 ± 5.8 Ma, with an MSWD of 0.0056 (Fig. 9b). Twenty analyses from sample TG-07-03 vary between 564 and 588 Ma, yielding a concordia age of 575.1 ± 3.6, with an MSDW of 0.15 (Fig. 9c).

We performed 380 analyses in as many zircon grains from the three Cap de Creus samples selected. We rejected 101 analyses with discordance higher than 10 %. The inherited component in these samples is also significant, and the resulting ages vary between 543 and 2,554 Ma. As in the previous samples, we selected the analyses younger than 590 Ma to extract the crystallization ages, whereas older data were regarded as inheritance. Zircons from the Cap de Creus samples display an assortment of textures under CL (Fig. 8b) that include abundant core-rim features with variable luminescence, where cores represent xenocrysts and are surrounded by oscillatory rims of magmatic origin (e.g., grains a19, b13 and c31 from sample CC-08-01 and grain c41 from sample CC-08-07 in Fig. 8b). Other textures comprise some homogeneous (e.g., grains a28, a35 and b9 from sample CC-08-08 in Fig. 8b) and scarce sector zoning (e.g., grain a22 from sample CC-08-07 in Fig. 8b).

In sample CC-08-01, twelve analyses vary between 568 and 590 Ma, yielding a concordia age (sensu Ludwig 1998) of 576.6 ± 2.7 Ma (Fig. 10a), with an MSWD of 0.23. In sample CC-08-07, twenty-two analyses vary between 543 and 590 Ma, yielding a concordia age of 571 ± 5 Ma (Fig. 10b). However, the high mean square of weighted deviation (MSWD = 10) suggests that more than one age

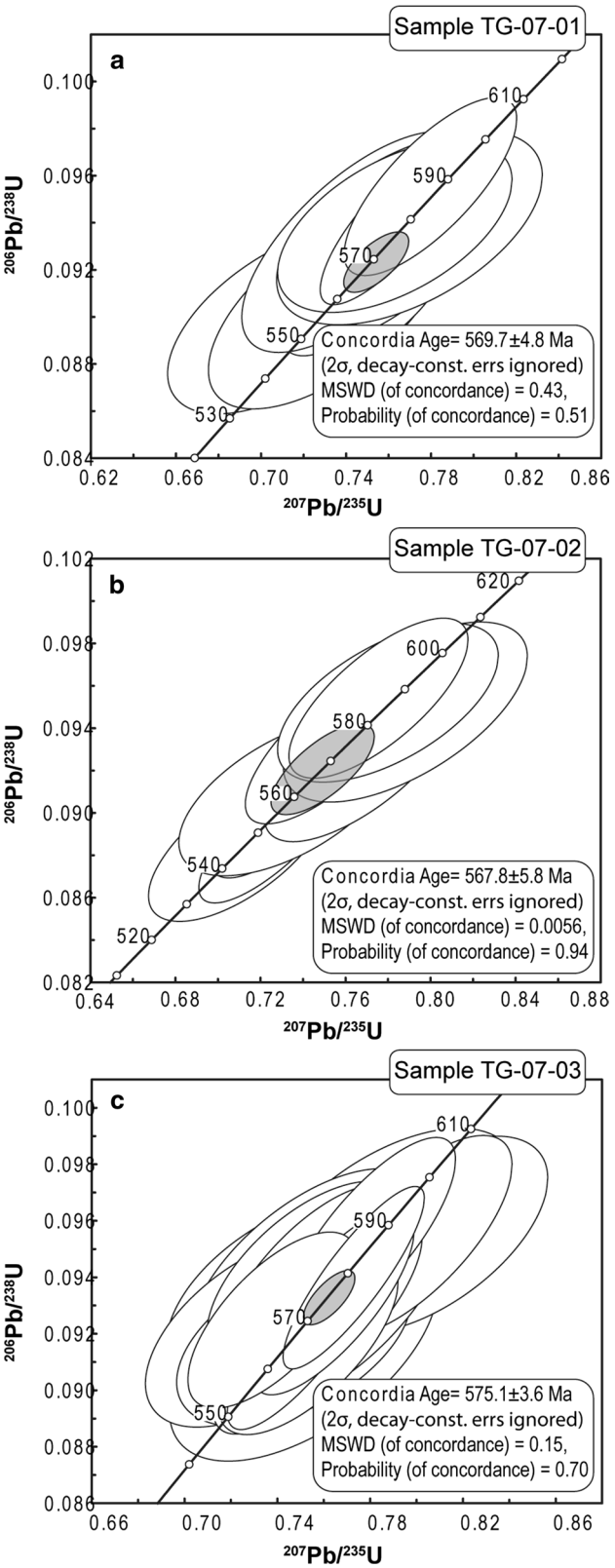

Fig. 9 Wetherill concordia diagrams for the Canigó samples **a** TG-07-01, **b** TG-07-02 and **c** TG-07-03. *Error ellipses* are plotted at 2σ

population is included in this concordant dataset. For this reason, we use the Sambridge and Compston (1994) statistical approach to extract these age populations. Thus, two classes can be established, namely an older age of 580 Ma and a younger age of 561 Ma (Fig. 10c). In order to decide between these two possible ages, we examine the CL images, where we can observe the disparity of CL textures in the oldest spots, (e.g., grains a22, a38 and c41 from sample CC-08-07 in Fig. 8b), whereas the areas that yielded the youngest ages show similar CL characteristics. Thus, we obtain a crystallization age of 563.2 ± 4.5 Ma (MSWD = 4.2) for this rock using the fourteen youngest analyses (Fig. 10b). Finally, twenty-seven analyses from sample CC-08-08 vary between 539 and 579 Ma, yielding a concordia age of 557.9 ± 3.0 Ma, with an MSDW of 2.8 (Fig. 10d).

Discussion

Petrogenesis, tectonic setting and age

The homogeneous patterns shown in the ORG-normalized trace element and in the chondrite-normalized REE diagrams suggest that all the samples were formed in the same tectonic setting. Furthermore, the high potassium content, the relative enrichment in large ion lithophile elements together with the HFSE content similar to that of arc granites and the Nb–Ta negative anomaly indicate that this setting was an active continental margin.

However, the whole-rock and isotope geochemistry of the samples reveal a subtle difference in their petrogenesis. On one hand, the enrichment in εNd registered in the Canigó samples (TG-07-01, 02 and 03), together with the absence of zircon-inherited ages (e.g., Cocherie et al. 2005; Castiñeiras et al. 2008) equivalent to the TDM ages (~1.5 Ga, Fig. 7), support the proposed tectonic setting, highlighting the variable influence of old material in a juvenile Neoproterozoic crust. This variable mixing of crustal components has been described in other areas of the European Variscan Belt, for instance in the Bohemian Massif, where felsic igneous rocks provide εNd values between −3.3 and −7.9 (−3.3 to −5.0, Linnemann and Romer 2002; −4.9 to −7.9, Mingram et al. 2004). These authors interpret the corresponding Mesoproterozoic TDM ages (between 1.6 and 1.9 Ga) as the result of the mixing of Paleoproterozoic–Archean and Neoproterozoic crustal portions. Our U–Pb ages obtained from zircon are equivalent within error in all the samples and indicate that the magmatism in the Canigó massif took place around 570 Ma. On the other hand, the Cap de Creus samples (CC-08-01, 07 and 08) show some differences among them, not only

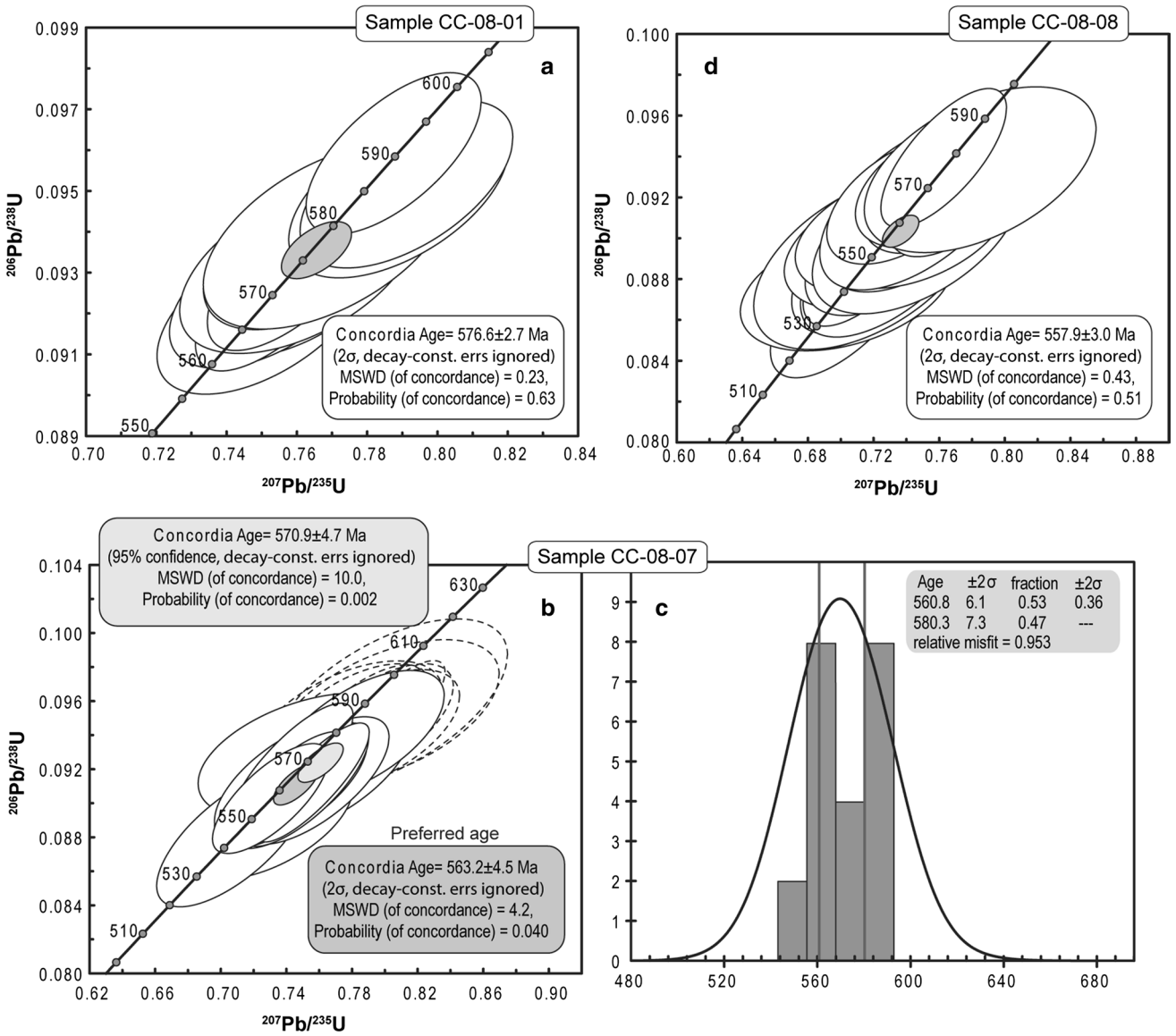

Fig. 10 U–Pb results for the Cap de Creus samples; **a**, **b** and **d** Wetherill concordia diagrams for samples CC-08-01, CC-08-07 and CC-08-08, **c** probability density plot showing the results of the Sambridge and Compston (1994) algorithm for sample CC-08-07 (see text for explanation). *Error ellipses* are plotted at 2*σ*

in their petrography and chemistry but also in their age. The presence of both amphibole and ignimbritic fiammes in samples CC-07-01 and CC-07-07 suggest some relationship with the metabasites found in the series, whereas sample CC-07-08 lacks amphibole. Moreover, their low REE content and the more depleted εNd values, particularly in sample CC-08-01 (εNd, −0.3), suggest variable proportions of interaction between mantle and old recycled continental crust. The ages obtained in these rocks are less homogeneous than in the Canigó, varying between 557.9 ± 3.0 and 576.6 ± 2.7 Ma. This combination of petrography, geochemistry and age suggests that the mantle influence may decrease with time. This evolution might be compatible both with the closure of an oceanic domain or with the thickening of a previous thinned crust, probably in a back-arc setting, where the influence of old crustal material is higher. The absence of ophiolites in the Ediacaran section of the Pyrenees and the abundance of coeval mafic lavas interbedded in the Ediacaran series of the Cap de Creus massif (Navidad and Carreras 1995) favor the latter possibility.

With the available data, it is not clear whether this juvenile influence is restricted to the Cap de Creus massif or whether it also affected the magmatism in the Canigó massif. If the former option were correct, both massifs would represent two slightly different scenarios in the active

continental margin, a small back-arc basin (Cap de Creus) and a zone with more continental influence (Canigó). Further studies on the influence of a juvenile source are necessary in the Canigó massif to either confirm or reject this interpretation.

An additional contribution of this work is the refinement in the age of the Ediacaran magmatism. The data presented here as well as previous published data provide evidence of an Ediacaran magmatic event lasting 30 Ma in NE Iberia. In this area, volcanic activity seems to be continuous from 577 (this work) to 548 Ma (Castiñeiras et al. 2008), whereas granite production took place between 560 and 553 Ma (Castiñeiras et al. 2008). Earlier studies (Cocherie et al. 2005; Castiñeiras et al. 2008) report ages obtained by SHRIMP using a limited amount of data (less than 25 analyses in each work). However, the abundance of inherited zircons in these volcaniclastic rocks hampers the interpretation of the preferred age in these studies. In fact, there is a variation of ~20 Ma from one work to another. Furthermore, even if the best smoothest zircon grains are selected to avoid detrital or inherited components in areas where a protracted active margin exists, zircons formed during the last magmatic event are not easy to distinguish from short-travelled zircons from closer and slightly older domains. In this case, the number of analyses should be increased to obtain a more reliable and representative set of the youngest population, which is interpreted as the age of magmatism. Given its higher velocity when compared with the SHRIMP technique, the LA-ICP-MS is the ideal choice to accomplish the task.

Our data also constrain the depositional age of the Late Neoproterozoic succession in the Cap de Creus and Canigó massifs. In the Cap de Creus massif, depositional ages range from 577 to 558 Ma, whereas the age obtained for the metavolcanic rocks of the Canigó massif (575–568 Ma) should be regarded as the minimum because of a thick series cropping out below these rocks. It should be noted that these ages were only obtained in felsic rocks and that the age of the protoliths of the metabasites is still unknown. However, we can consider a similar Late Neoproterozoic age for the metabasaltic lava flows interbedded in the lower part of the succession although the protolith age of the plutonic metabasites remains unresolved and a younger pre-Variscan (Ordovician?) age cannot be ruled out. Further geochemical and geochronological studies are warranted to elucidate this problem.

Comparison with neighboring areas

This magmatism may be part of a longer cycle, as revealed by the distribution of magmatic ages obtained in neighboring areas. In the French Massif Central, a magmatic event ranging from Late Neoproterozoic (617 ± 17 Ma, Alexandre 2007; and 574 ± 28 Ma, Melleton et al. 2010) to Early Cambrian (525 ± 12 Ma, Alexandrov et al. 2001; 526 ± 14 Ma, Alexandre 2007; and 529 ± 4 Ma, Melleton et al. 2010) has been described in the metasedimentary successions of the different structural units. In the Montagne Noire, south of the French Massif Central, metavolcanic rocks provided an age of 545 ± 15 Ma for the "schistes X" in the uppermost part of the Late Neoproterozoic succession (Lescuyer and Cocherie 1992). These data reinforce the aforementioned correlation between the lowermost series of the Eastern Pyrenees and the Montagne Noire based on lithostratigraphic criteria (Cavet 1957) or on the strong similarities of the metallogenic assemblages (Ayora and Casas 1986). In the Iberian Massif, a magmatic cycle of a similar age has been described. In the Narcea Antiform, between the Cantabrian and Western Asturian-Leonese zones, Late Neoproterozoic ages ranging from 605 ± 10 to 557 ± 3 Ma for plutonic and volcanic rocks intruded or interlayered in the Neoproterozoic siliciclastic series have been obtained by Fernández-Suárez et al. (1998), Gutiérrez-Alonso et al. (2004) and Rubio-Ordónez et al. (2013). In the Ossa Morena zone, Bandrés et al. (2004) describe diorite and granite bodies intruding at 577.6 ± 0.6 and 573 ± 14 Ma. All these authors agree that this Late Neoproterozoic–Early Cambrian magmatism is related to a convergent margin setting, which is a subduction-related magmatic arc. In the Bohemian Massif, in the Saxo-Thuringian Zone and the Moldanubian Zone, a Late Neoproterozoic bimodal magmatism ranging from 549 ± 6 to 575 ± 4 and 600 ± 7 Ma is also exposed (Mingram et al. 2004; Teipel et al. 2004). In the Fore-Sudetic Block, two different thermal events produced zoned zircon overgrowth at ca. 600 and 568 Ma (Oberc-Dziedzic et al. 2003) and in the Sudetes, the Radzimowice Slates include major populations of zircons of Cadomian age, between 550 and 650 Ma (Tyszka et al. 2008).

A similar situation has been reported in other Mediterranean Variscan realms involved in the Alpine orogens. In the basement rocks of the Calabria–Peloritani Mountains (southern Italy and NE Sicily), Micheletti et al. (2007), Williams et al. (2012) and Fiannacca et al. (2013) describe an important Late Neoproterozoic–Early Cambrian magmatism ranging from 565 ± 5 to 526 ± 10 Ma. Based on the age of zircon cores, Williams et al. (2012) and Fiannacca et al. (2013) propose a proximity between the depositional age of the Neoproterozoic sequences and the age of the plutonic rocks, indicating a short time span between sedimentation and generation of granitic rocks. In the Menderes massif (western Taurides), Zlatkin et al. (2013) describe a similar situation: bimodal Late Neoproterozoic magmatic rocks intruded from 550.6 ± 1.1 to 544 Ma in a sequence that exhibits a very close sedimentation age from ~570 to 550 Ma. Finally, in the Late Neoproterozoic

basement rocks of the western Pontides, Yilmaz Şahin et al. (2013) reported granites with similar ages from 546 ± 3.9 to 534 ± 4.7 Ma.

Given the available geochronological and geochemical data and the results presented in this paper, it may be argued that the studied rocks record a fragment of a long-lived subduction-related magmatic arc (620–520 Ma) in the active northern Gondwana margin. This margin can be recognized in the Variscan belt of western and central Europe. Furthermore, the fragments of Ediacaran rocks recognized in the Mediterranean orogens suggest that the margin can be extended eastwards through the Turkish massif as far as the Iranian and Caucasus Mountains [see discussion in Yilmaz Şahin et al. (2013)].

The homogeneity shown by all these crustal fragments along the Gondwana margin indicates that the individualization of the Pyrenean basement with respect to the Iberian Massif would have started later, probably during its transition from an active to a passive margin in Cambro–Ordovician times.

Conclusions

The geochemistry of felsic metavolcanic rocks in the upper part of the Ediacaran series from the Canigó and Cap de Creus massifs indicates a convergent setting for their origin. In the Cap de Creus massif, isotope geochemistry suggests a juvenile influence in their petrogenesis whereas, in the Canigó massif, the crustal component is more important. The U–Pb ages obtained reveal that this volcanism took place around 570 Ma in the Canigó massif, but in Cap de Creus the volcanic event spanned from 558 to 577 Ma.

The rocks under study display characteristics similar to those of other Cadomian remnants found in the Variscan and Alpine basement, which taken together represent a convergent margin located in northern Gondwana from 620 through 520 Ma. The partition between the Pyrenean domain and the Iberian Massif probably occurred in Cambro–Ordovician times, when the tectonic setting underwent a transition from an active to a passive margin.

Acknowledgments This work was funded by projects CGL2010-21298 and Consolider-Ingenio 2010, under CSD2006-00041 "Topoiberia." Detailed comments of R. Kryza, the editor and an anonymous reviewer greatly improved a first version of the manuscript.

References

Aguilar C, Liesa M, Castiñeiras P, Navidad M (2013) Late Variscan metamorphic and magmatic evolution in the Eastern Pyrenees revealed by U–Pb age zircon dating. J Geol Soc Lond. doi:10.1144/jgs2012-086

Alexandre P (2007) U–Pb zircon SIMS ages from the French Massif Central and implication for the pre-Variscan tectonic evolution in Western Europe. Comptes Rendus Geosci 339:613–621

Alexandrov P, Floc'h J-P, Cuney M, Cheilletz A (2001) Datation U–Pb à la microsonde ionique des zircons de l'unité supérieure de gneiss dans le Sud Limousin, Massif central. Comptes Rendus de l'Académie des Sciences 332:625–632

Ayora C, Casas JM (1986) Strabound As–Au mineralization in pre-Caradocian rocks form the Vall de Ribes, Eastern Pyrenees, Spain. Miner Deposita 21:278–287

Bandrés A, Eguíluz L, Pin C, Paquette JL, Ordóñez B, Le Fèvre B, Ortega LA, Ibarguchi JIG (2004) The northern Ossa-Morena Cadomian batholith (Iberian Massif): magmatic arc origin and early evolution. Int J Earth Sci 93:860–885

Carignan J, Hild P, Mevelle G, Morel J, Yeghicheyan D (2001) Routine analyses of trace elements in geological samples using flow injection and low pressure on-line liquid chromatography coupled to ICP–MS; a study of geochemical reference materials BR, DR-N, UB-N, AN-G and GH. Geostand Newsl 25:187–198

Carreras J, Druguet E (2013) Illustrated field guide to the geology of cap de creus. Servei de Publicacions de la Universitat Autònoma de Barcelona

Carreras J, Ramírez J (1984) The geological significance of the Port de la Selva Gneisses (Eastern Pyrenees, Spain). IGCP Newsl 6:27–31

Casas JM (2010) Ordovician deformations in the Pyrenees: new insights into the significance of pre-Variscan ('sardic') tectonics. Geol Mag 147:674–689

Casas JM, Fernandez O (2007) On the Upper Ordovician unconformity in the Pyrenees: new evidence from the La Cerdanya area. Geol Acta 5:193–198

Casas JM, Palacios T (2012) First age data obtained by Acritarchs in the pre-Upper Ordovician sequences of the Pyrenees: on the late Cambrian-early Ordocivian age of the Jujols Series. Comptes Rendus Geosci 344:50–56

Casas JM, Martí J, Ayora C (1986) Importance du volcanisme dans la composition lithostratigraphique du Paléozoïque inférieur des Pyrénées catalanes. Comptes Rendus de l'Académie des Sciences 302:1193–1198

Casas JM, Castiñeiras P, Navidad M, Liesa M, Carreras J (2010) New insights into the Late Ordovician magmatism in the Eastern Pyrenees: U–Pb SHRIMP zircon data from the Canigó massif. Gondwana Res 17:317–324

Castiñeiras P, Navidad M, Liesa M, Carreras J, Casas JM (2008) U–Pb zircon ages (SHRIMP) for Cadomian and Lower Ordovician magmatism in the Eastern Pyrenees: new insights in the pre-Variscan evolution of the northern Gondwana margin. Tectonophysics 46:228–239

Cavet P (1957) Le Paléozoïque de la zone axiale des Pyrénées orientales françaises entre le Roussillon et l'Andorre. Bull Serv Carte Géol Fr 55:303–518

Cirés J, Casas JM, Santanach P, Muñoz JA, Fleta J, Serrat D (1994) Mapa geológico de España (1:50.000): Molló (no 218). ITGE Madrid, España

Cocherie A, Baudin T, Autran A, Guerrot C, Fanning CM, Laumonier B (2005) U–Pb zircon (ID-TIMS and SHRIMP) evidence for the early Ordovician intrusion of metagranites in the late Proterozoic Canaveilles Group of the Pyrenees and the Montagne Noire (France). Bulletin de la Société Géologique de France 176:269–282

Den Brok SWJ (1989) Evidence for pre-Variscan deformation in the Lys Caillaouas area, Central Pyrenees, France. Geol Mijnbouw 68:377–380

DePaolo DJ (1981) Neodymiun isotopes in the Colorado Front range and crust-mantle evolution in the Proterozoic. Nature 291:193–196

Eguiluz L, Ibarguchi JIG, Ábalos B, Apraiz A (2000) Superposed Hercynian and Cadomian orogenic cycles in the Ossa-Morena zone and related areas of the Iberian Massif. Geol Soc Am Bull 112:1398–1413. doi:10.1130/0016-7606(2000)112<1398:SHACOC>2.0.CO;2

Fernández-Suárez J, Gutiérrez Alonso G, Jenner G, Simon EJ (1998) Geochronology and geochemistry of the Pola de Allande granitoids (northern Spain): their bearing on the Cadomian–Avalonian evolution of northwest Iberia. Can J Earth Sci 35:1439–1453

Fiannacca P, Williams IS, Cirrincione R, Pezzino A (2013) The augen gneisses of the Peloritani Mountains (NE Sicily): Granitoid magma production during rapid evolution of the northern Gondwana margin at the end of the Precambrian. Gondwana Res 23:782–796. doi:10.1016/j.gr.2012.05.019

Frei D, Gerdes A (2009) Precise and accurate in situ U–Pb dating of zircon with high sample throughput by automated LA–SF–ICP–MS. Chem Geol 261:261–270

García-Sansegundo J, Alonso JL (1989) Stratigraphy and structure of the southeastern Garona Dome. Geodin Acta 3:127–134

Gerdes A, Zeh A (2006) Combined U–Pb and Hf isotope LA–(MC–)ICP–MS analysis of detrital zircons: comparison with SHRIMP and new constraints for the provenance and age of an Armorican metasediment in Central Germany. Earth Planet Sci Lett 249:47–61

Guitard G (1970) Le métamorphisme hercynien mésozonal et les gneiss oeillés du massif du Canigou (Pyrénées orientales). Mémoires du B.R.G.M. 63

Guitard G, Laffitte F (1956) Sur l'importance et la nature des manifestations volcaniques dans le Paléozoïque des Pyrénées Orientales. Comptes Rendus de l'Académie des Sciences 242:2749–2752

Gutiérrez-Alonso G, Fernández-Suárez J, Jeffries TE (2004) Age and setting of the Upper Neoproterozoic Narcea Antiform volcanic rocks. Geogaceta 25:79–82

Harris NBW, Pearce JA, Tindle AG (1986) Geochemical characteristics of collision-zone magmatism. In: Coward MP, Ries AC (eds) Collision tectonics. Geological Society Special Publication 19, pp 67–81

Hartevelt JJA (1970) Geology of the upper Segre and Valira valleys, central Pyrenees, Andorra/Spain. Leidse Geol Meded 45:167–236

Hastie AR, Kerr AC, Pearce JA, Mitchell SF (2007) Classification of altered volcanic island arc rocks using immobile trace elements: development of the Th–Co discrimination diagram. J Petrol 48:2341–2357. doi:10.1093/petrology/egm062

Jacobsen SB, Wasseburg GJ (1980) Sm–Nd isotopic evolution of chondrites. Earth Planet Sci Lett 50:139–155

Kriegsman LM, Aerden DGAM, Bakker RJ, den Brok SWJ, Schutjens PMTM (1989) Variscan tectonometamorphic evolution of the eastern Lys-Caillaouas massif, Central Pyrenees-evidence for late orogenic extension prior to peak metamorphism. Geol Mijnbouw 68:323–333

Laumonier B, Guitard G (1986) Le Paléozoïque inférieur de la moitié orientale de la Zone Axiale des Pyrénées. Essai de synthèse. Comptes Rendus de l'Académie Sciences Paris 302:473–478

Lescuyer JL, Cocherie A (1992) Datation sur monozircons des métadacites de Sériès: arguments pour un âge protérozoïque terminal des schistes X de la Montagne Noire (Massif central français). Comptes Rendus de l'Académie des Sciences 314:1071–1077

Linnemann U, Romer RL (2002) The Cadomian Orogeny in Saxo-Thuringia, Germany: geochemical and Nd–Sr–Pb isotopic characterization of marginal basins with constraints to geotectonic setting and provenance. Tectonophysics 352:33–64

Linnemann U, Gerdes A, Drost K, Buschmann B (2007) The continuum between Cadomian orogenesis and opening of the Rheic Ocean: constraints from LA–ICP–MS U–Pb zircon dating and analysis of plate-tectonic setting (Saxo-Thuringian zone, northeastern Bohemian Massif, Germany). In: Linnemann U, Nance RD, Kraft P, Zulauf G (eds) The evolution of the Rheic Ocean: from Avalonian–Cadomian active margin to Alleghenian-Variscan collision: Geological Society of America Special Paper 423, pp 61–96. doi:10.1130/2007.2423(03)

Linnemann U, Gerdes A, Hofmann M, Marko L (2014) The Cadomian Orogen: Neoproterozoic to Early Cambrian crustal growth and orogenic zoning along the periphery of the West African Craton–Constraints from U–Pb zircon ages and Hf isotopes (Schwarzburg Antiform, Germany). Precambrian Res (in press). doi:10.1016/j.precamres.2013.08.007

Losantos M, Palau J, Carreras J, Druguet E, Santanach P, Cirés J (1997) Mapa geològic de Catalunya, Escala 1:25.000 Fulls: Roses 259-1-1, Cap de Creus, 259-2-1, Far de Roses 259-1-2. ICC Barcelona, España

Ludwig KR (1998) On the treatment of concordant uranium-lead ages. Geochim Cosmochim Acta 62:665–676

Ludwig KR (2001) Users manual for isoplot/Ex rev. 2.49. Berkeley Geochronology Center Special Publication No. 1a, pp 1–56

Maurel O, Respaut JP, Monié P, Arnaud N, Brunel M (2004) U–Pb emplacement and 40Ar/39Ar cooling ages of the eastern Mont-Louis granite massif (Eastern Pyrenees, France). Comptes Rendus Geosci 336:1091–1098

Melleton J, Cocherie A, Faure M, Rossi P (2010) Precambrian protoliths and Early Paleozoic magmatism in the French Massif Central: U–Pb data and the North Gondwana connection in the west European Variscan belt. Gondwana Res 17:13–25. doi:10.1016/j.gr.2009.05.007

Mezger JE (2010) Cadomian, Ordovician and Variscan igneous events preserved in gneiss domes of the Central Pyrenean Axial Zone. 13. Symposium "Tektonik, Struktur- und Kristallingeologie" (TSK 13), Frankfurt, 6–12 April 2010. TSK 13 conference abstracts and field guides, 40

Micheletti F, Barbey P, Fornelli A, Piccarreta G, Deloule E (2007) Latest Precambrian to Early Cambrian U–Pb zircon ages of augen gneisses from Calabria (Italy), with inference to the Alboran microplate in the evolution of the peri-Gondwana terranes. Int J Earth Sci 96:843–860. doi:10.1007/s00531-006-0136-0

Mingram B, Kröner A, Hegner E, Krentz O (2004) Zircon ages, geochemistry, and Nd isotopic systematics of pre-Variscan orthogneisses from the Erzgebirge, Saxony (Germany), and geodynamic interpretation. Int J Earth Sci 93:706–727

Muñoz JA (1992) Evolution of a continental colision belt:ECORS-Pyrenees crustal balanced cross-section. In: McClay KR (ed) Thrust tectonics. Chapman & Hall, London, pp 235–246

Muñoz JA, Vergés J, Martínez-Rius A, Fleta J, Cirés J, Casas JM, Sàbat F (1994) Mapa geológico de España (1:50.000): Ripoll (no 256). ITGE Madrid, España

Murphy JB, Pisarevsky SA, Nance RD, Keppie JD (2004) Neoproterozoic-early Paleozoic evolution of peri-Gondwanan terranes: implications for Laurentia–Gondwana connections. Int J Earth Sci 93:659–682. doi:10.1007/s00531-004-0412-9

Nance RD, Gutiérrez-Alonso G, Keppie JD, Linneman U, Murphy JB, Quesada C, Strahan RA, Woodcock NH (2010) Evolution of the Rheic Ocean. Gondwana Res 17:194–222

Navidad M, Carreras J (1995) Pre-Hercynian magmatism in the Eastern Pyrenees (Cap de Creus and Albera Massifs) and its geodynamical setting. Geol Mijnbouw 74:65–77

Navidad M, Carreras J (2002) El volcanismo de la base del Paleozoico Inferior del Canigó (Pirineos Orientales). Evidencias geoquímicas de la apertura de una cuenca continental. Geogaceta 32:91–94

Navidad M, Castiñeiras P, Casas JM, Liesa M, Fernández Suárez J, Barnolas A, Carreras J, Gil-Peña I (2010) Geochemical characterization and isotopic age of Caradocian magmatism in the northeastern Iberian Peninsula: insights into the Late Ordovician evolution of the northern Gondwana margin. Gondwana Res 17:325–337

Neubauer F (2002) Evolution of late Neoproterozoic to early Paleozoic tectonic elements in Central and Southeast European Alpine mountain belts: review and synthesis. Tectonophysics 352:87–103. doi:10.1016/S0040-1951(02)00190-7

Oberc-Dziedzic T, Klimas K, Kryza R, Fanning CM (2003) SHRIMP U–Pb zircon geochronology of the Strzelin gneiss, SW Poland: evidence for a Neoproterozoic thermal event in the Fore-Sudetic Block, Central European Variscides. Int J Earth Sci 92:701–711

Pearce JA, Harris NGW, Tindle AG (1984) Trace element discrimination diagrams for the tectonic interpretation of granitic rocks. J Petrol 25:956–983. doi:10.1093/petrology/25.4.956

Rodríguez-Alonso MD, Peinado M, López-Plaza M, Franco P, Carnicero A, Gonzalo JC (2004) Neoproterozoic–Cambrian synsedimentary magmatism in the Central Iberian Zone (Spain): geology, petrology and geodynamic significance. Int J Earth Sci 93:897–920

Romer RL, Soler A (1995) U–Pb age and lead isotopic characterization of Au-bearing skarn related to the Andorra granite. Miner Deposita 30:374–383

Rubio-Ordónez A, Gutiérrez-Alonso G, Valverde-Vaquero P, Cuesta A, Gallastegui G, Gerdes A, Cárdenes V (2013) Arc-related Ediacaran magmatism along the northern margin of Gondwana: geochronology and isotopic geochemistry from northern Iberia. Gondwana Res (in press). doi:10.1016/j.gr.2013.09.016

Sambridge MS, Compston W (1994) Mixture modeling of multi-component data sets with application to ion-probe zircon ages. Earth Planet Sci Lett 128:373–390

Santanach PF (1972a) Sobre una discordancia en el Paleozoico inferior de los Pirineos orientales. Acta Geológica Hispánica 7:129–132

Santanach PF (1972b) Estudio tectónico del Paleozoico inferior del Pirineo entre la Cerdaña y el río Ter. Acta Geológica Hispánica 7:44–49

Simancas JF, Expósito I, Azor A, Martínez Poyatos D, González Lodeiro F (2004) From the Cadomian orogenesis to the Early Paleozoic Variscan rifting in Southwest Iberia. J Iberian Geol 30:53–71

Stacey JS, Kramers JD (1975) Approximation of terrestrial lead isotope evolution by a two-stage model. Earth Planet Sci Lett 26:207–221

Steiger RH, Jäger E (1977) Subcomission on geochronology: convention on the use of decay constants in geo- and cosmochronology. Earth Planet Sci Lett 36:359–362

Talavera C, Montero P, Martínez Poyatos D, Williams IS (2012) Ediacaran to Lower Ordovician age for rocks ascribed to the Schist–Graywacke complex (Iberian Massif, Spain): evidence from detrital zircon SHRIMP U–Pb geochronology. Gondwana Res 22:928–942

Taylor SR, McLennan SM (1985) The continental crust: its composition and evolution. Blackwell, Oxford

Teipel U, Eichhorn R, Loth G, Rohrmüller J, Höll R, Kennedy A (2004) U–Pb SHRIMP and Nd isotopic data from the western Bohemian Massif (Bayerischer Wald, Germany): implications for Upper Vendian and Lower Ordovician magmatism. Int J Earth Sci 93:782–801

Tyszka R, Kryza R, Zalasiewic JA, Larionov AN (2008) Multiple Archaean to Early Palaeozoic events of the northern Gondwana margin witnessed by detrital zircons from the Radzimowice Slates, Kaczawa Complex (Central European Variscides). Geol Magazime 145:85–93

Williams IS, Fiannacca P, Cirrincione R, Pezzino A (2012) Peri-Gondwanan origin and early geodynamic history of NE Sicily: a zircon tale from the basement of the Peloritani Mountains. Gondwana Res 22:855–865. doi:10.1016/j.gr.2011.12.007

Winchester JA, Floyd PA (1977) Geochemical discrimination of different magma series and their differentiation products using immobile elements. Chem Geol 20:325–343

Yilmaz Şahin S, Aysal N, Güngör Y, Peytcheva I, Neubauer F (2013) Geochemistry and U–Pb zircon geochronology of metagranites in Istranca (Strandja) Zone, NW Pontides, Turkey: implications for the geodynamic evolution of Cadomian orogeny. Gondwana Res (in press). doi:10.106/j.gr.2013.07.011

Zlatkin O, Avigad D, Gerdes A (2013) Evolution and provenance of Neoproterozoic basement and Lower Paleozoic siliciclastic cover of the Menderes Massif (western Taurides): coupled U–Pb–Hf zircon isotope geochemistry. Gondwana Res 23:682–700

Zwart HJ (1979) The geology of the central Pyrenees. Leidse Geol Meded 50:1–74